

Supplement of The Cryosphere, 14, 1703–1712, 2020  
<https://doi.org/10.5194/tc-14-1703-2020-supplement>  
© Author(s) 2020. This work is distributed under  
the Creative Commons Attribution 4.0 License.



*Supplement of*

## **Horizontal ice flow impacts the firm structure of Greenland’s percolation zone**

**Rosemary Leone et al.**

*Correspondence to:* Joel Harper ([joel@mso.umt.edu](mailto:joel@mso.umt.edu))

The copyright of individual parts of the supplement might differ from the CC BY 4.0 License.

## S1. Model Limitations

### S1.1 Neglect of along-flow velocity variations

Our model includes the role of changing surface velocities on the surface boundary condition as the firn column is transported through the percolation zone. However, along-flow velocity changes may also influence densification rates by 1) introducing longitudinal deviatoric stresses that increase the effective stress, and therefore strain and densification rates within the firn profile, and 2) change the rate at which mass is added to the firn column through strain thickening/thinning. These mechanisms are not included in our modeling approach.

10

Mechanism 1 has been found to heavily influence density structure in the special case of Antarctic ice streams (Alley and Bentley, 1988), but we expect this enhanced softening to be negligibly important in Greenland's percolation zone for two reasons: 1) firn temperatures in the percolation zone are relatively warm (cf. Antarctica) as a result of meltwater infiltration and refreezing. The warmer temperatures will decrease the firn viscosity, thereby limiting longitudinal deviatoric stresses. 2) Longitudinal deviatoric stresses are a function of the 2<sup>nd</sup> derivative of the velocity. Over the vast majority of Greenland's percolation zone, small velocity variations result in 2<sup>nd</sup> derivatives that are essentially negligible. As one example, Meierbachtol et al. (2016) found longitudinal resistive stresses to be very small above the long term ELA around the K-Transect.

20

Regarding mechanism 2, the Herron and Langway assumptions upon which our model is based, assume that the densification rate is a function of the current density, and the rate

at which mass is added (this is the accumulation rate). This is given as:  $\frac{d\rho}{dt} =$

25  $C(\rho_i - \rho)b\rho_i$  (note that in Herron and Langway the constant C absorbs ice density so the equation becomes  $\frac{d\rho}{dt} = k(\rho_i - \rho)$ , eg. Reeh et al. (2005). The addition or removal of mass from ice flow effectively acts to modify the mass addition from accumulation. The magnitude of this mass gain/loss depends on depth in the firm column. Deeper in the column, the mass gain/loss is amplified because the horizontal straining is acting over a  
30 larger firm thickness. The addition of a strain thinning/thickening term can be included in the equation for densification rate as:

$\frac{d\rho}{dt} = C(\rho_i - \rho) \left( b\rho_i - \dot{\epsilon}_{xx} \int_{sfc}^z \rho(z) dz \right)$ . For clarity, we simplify the integral so that the equation reads:  $\frac{d\rho}{dt} = C(\rho_i - \rho) \left( b\rho_i - \dot{\epsilon}_{xx} \overline{z\rho(z)} \right)$ . The horizontal strain is positive in stretching, and the variable z refers to the depth below the surface.

35

The above equation provides a convenient way to think about the influence of velocity variations on densification. Over the vast majority of the ice sheet, accumulation rates are on the order  $10^{-1}$ - $10^0$  m a<sup>-1</sup> (ice equivalent). In contrast, strain rates over the vast majority of the GrIS percolation zone are exceeding small. Horizontal strain rates are on the order  
40  $10^{-3}$  -  $10^{-4}$  a<sup>-1</sup> (for instance, EGIG and K-transect flowlines show velocities which increase by <50 m a<sup>-1</sup> over the *lowest* 50 km; a strain rate of <10<sup>-3</sup> a<sup>-1</sup>). When integrated over 10s of m of firm, the thinning rates are unlikely to exceed  $\sim 10^{-2}$  m a<sup>-1</sup>: a small fraction of accumulation.

45 While the above argument holds for the vast majority of the ice sheet, there are rare regions where large speed-ups along the flowline result in substantial longitudinal stretching rates. The Jakobshavn transect is one such location. Horizontal strain rates are on the order  $\sim 10^{-2} \text{ a}^{-1}$  in the lowest reaches of the transect. For a firn thickness of  $\sim 30 \text{ m}$  (Figure 3) with average density  $\sim 600 \text{ m kg}^{-3}$ , the resulting mass loss from thinning offset  
 50 as much as  $\sim 40\%$  of accumulation. However, in these rare locations, crevassing is likely to take up the majority of the strain, minimizing the continuous mass loss from strain thinning. This is indeed the case along Jakobshavn and even EGIG, where extensive crevassing has occurred in recent years, limiting the mobility of field parties (including ours).

55

### **S1.2 Quantifying the consequences of neglecting horizontal diffusion**

To assess the consequences of neglecting horizontal heat diffusion in our modeling scheme, we developed an explicit 2D model for densification and heat transport for testing. In this formulation, we include the horizontal term along the flow direction in  
 60 Equation 1, so that 2D firn densification is defined as:

$$\frac{D\rho}{Dt} = \frac{\partial\rho}{\partial t} + w\frac{\partial\rho}{\partial z} + u\frac{\partial\rho}{\partial x} \quad (\text{S1})$$

where  $u$  corresponds to the horizontal velocity. The temperature equation was also updated to include horizontal advection terms:

$$\rho c \frac{\partial T}{\partial t} = k_T \left( \frac{\partial^2 T}{\partial z^2} + \frac{\partial^2 T}{\partial x^2} \right) - \rho c u \frac{\partial T}{\partial x} + \left[ \frac{dk_T}{dz} - \rho c w \right] \frac{\partial T}{\partial z} \quad (\text{S2})$$

The surface boundary condition for temperature varied by several degrees across the surface domain to simulate the lower elevations of the percolation zone.

65 This explicit two dimensional framework and our Lagrangian scheme, which includes horizontal advection impacts on densification and heat transfer, but not diffusion, were tested over a 90 km model domain, with a constant accumulation rate of 0.5 m a<sup>-1</sup>. Surface temperature varied from -19 to -13 over the model domain, in approximate agreement with observations along the EGIG transect. Model simulations  
70 were executed with a prescribed surface velocity of 100 m a<sup>-1</sup>, which approximates conditions along the EGIG transect, and with a surface velocity of 1000 m a<sup>-1</sup> to test the consequences of neglecting horizontal diffusion under an extreme scenario.

Comparison of results for the 100 m a<sup>-1</sup> scenario are presented in Figure S1. The consequences of neglecting horizontal diffusion are negligible for both density and  
75 temperature results. Neglecting horizontal diffusion is more consequential under high surface velocity. But even under surface speeds of 1000 m a<sup>-1</sup>, conditions which can be considered extreme for the percolation zone, the maximum temperature difference is ~0.15°C; a difference which has negligible impact on modeled density. This supports our modified approach, which we use for its flexible implementation of melt schemes and its  
80 fast run time.

## S2. Sensitivity Testing

Model results including horizontal advection were compared against 1D steady state results at the lower end of the model domain. We used temperature at pore close off and  
85 total air content as comparison metrics. The cumulative air content in meters ice equivalent is the integrated difference between infiltration ice density and firn density:

$$C(z) = \frac{1}{\rho_{ii}} \int_0^z (\rho_{ii}(\zeta) - \rho(\zeta)) d\zeta \quad (S3)$$

where  $\rho$  is firn density and  $\rho_{ii}$  is infiltration ice density, and  $z$  is depth. We used an average density of  $843 \text{ kg m}^{-3}$  for infiltration ice (Harper et al., 2012). This calculation does not take into account perennial firn aquifers where capacity must be adjusted by 8.9% due to density differences between water and ice (Koenig et al., 2014).

Both 2D and 1D model simulations were performed for each sensitivity scenario, and the difference was calculated as a percentage:

$$\sigma_{\%diff} = \frac{\sigma_{2D} - \sigma_{1D}}{\left(\frac{\sigma_{1D} + \sigma_{2D}}{2}\right)} \quad (\text{S4})$$

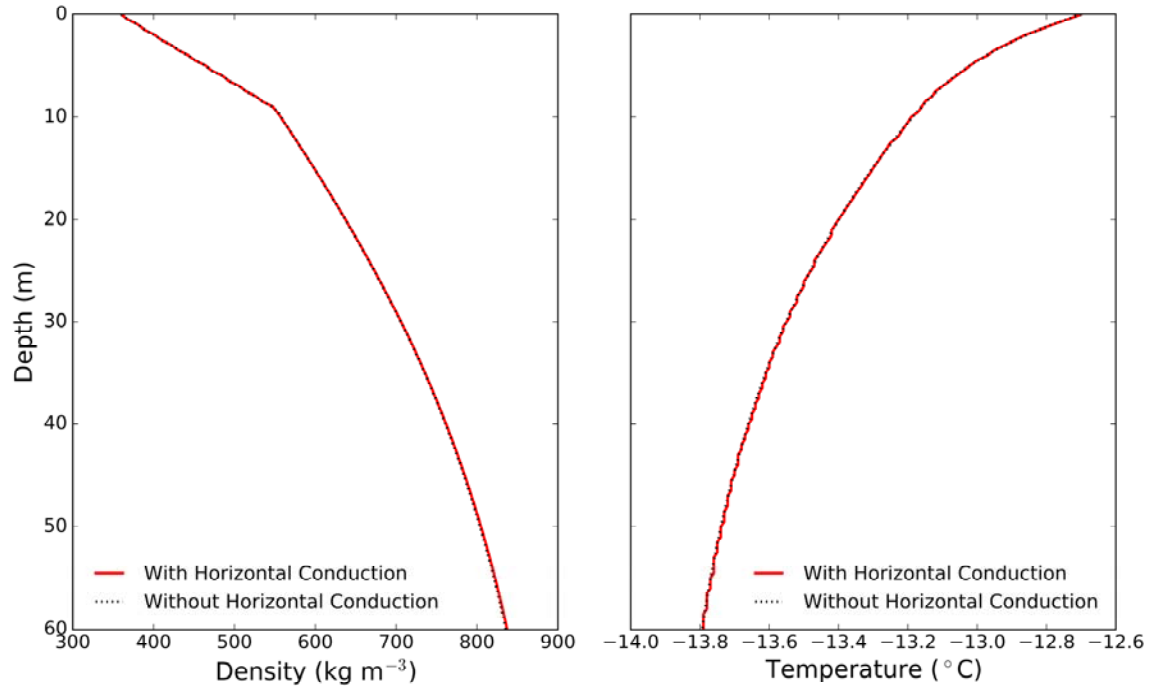
where  $\sigma$  is the metric of interest. Note that given this formulation, because firn temperatures are never  $>0^\circ\text{C}$ , the denominator in S9 is negative and so temperatures in 2D simulations that are colder than the 1D counterpart reflect a positive difference.

### **S3. Model Results along GrIS Transects Under Different Melt Infiltration Schemes**

The influence of horizontal ice flow on firn density and temperature is explored over 4 different GrIS transects. The difference between 2D and 1D model results is calculated as:

$$\sigma_{diff} = \sigma_{2D} - \sigma_{1D} \quad (\text{S5})$$

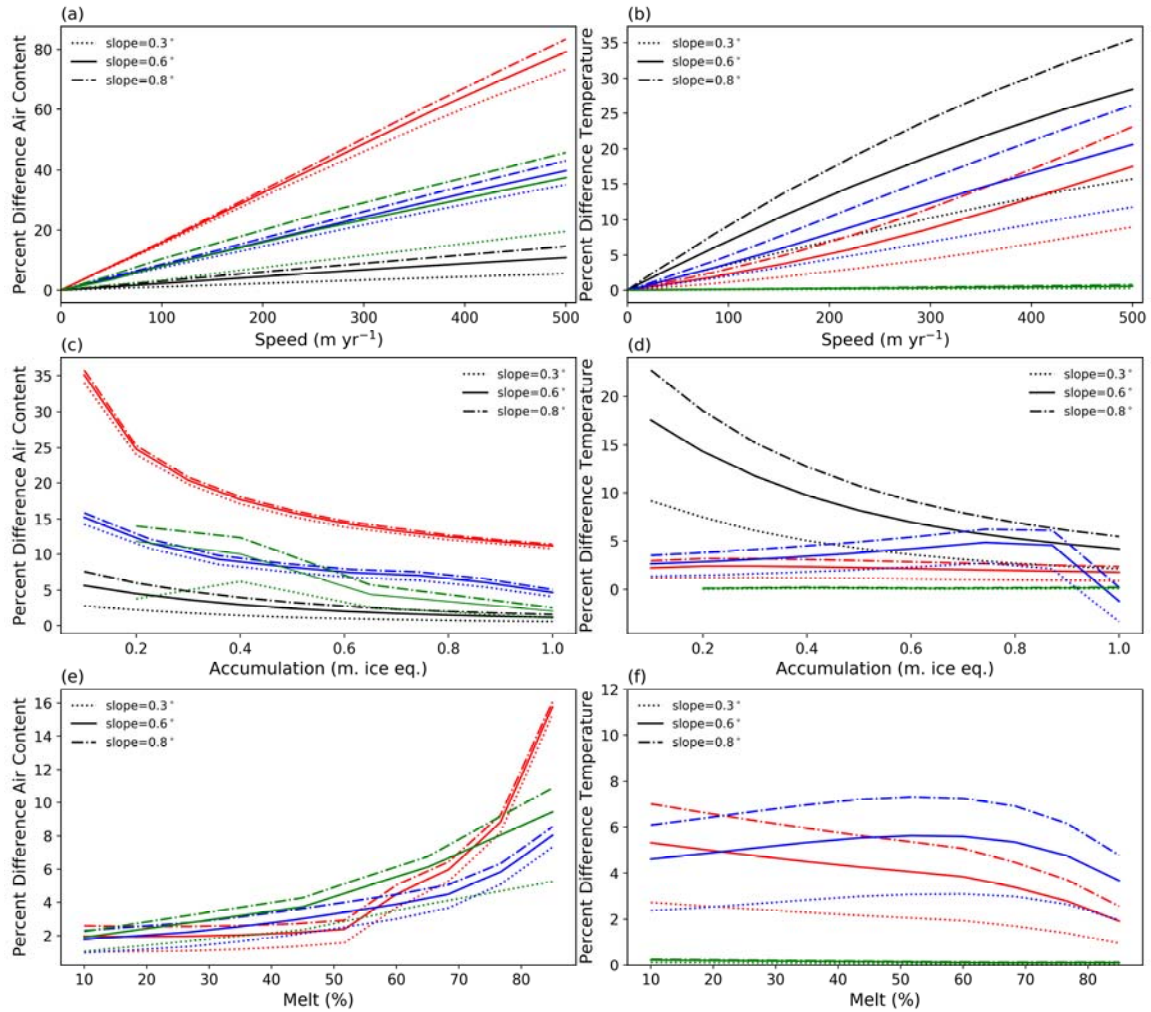
where  $\sigma$  is the metric of interest. Figure S3 shows surface conditions; Figure S4 and S5 present results for the Reeh et al. (2005) and continuum meltwater infiltration schemes.



105 **Figure S1.** Simulated density (A) and temperature (B) results 80 km from the inland  
 model boundary with, and without horizontal heat conduction.

110

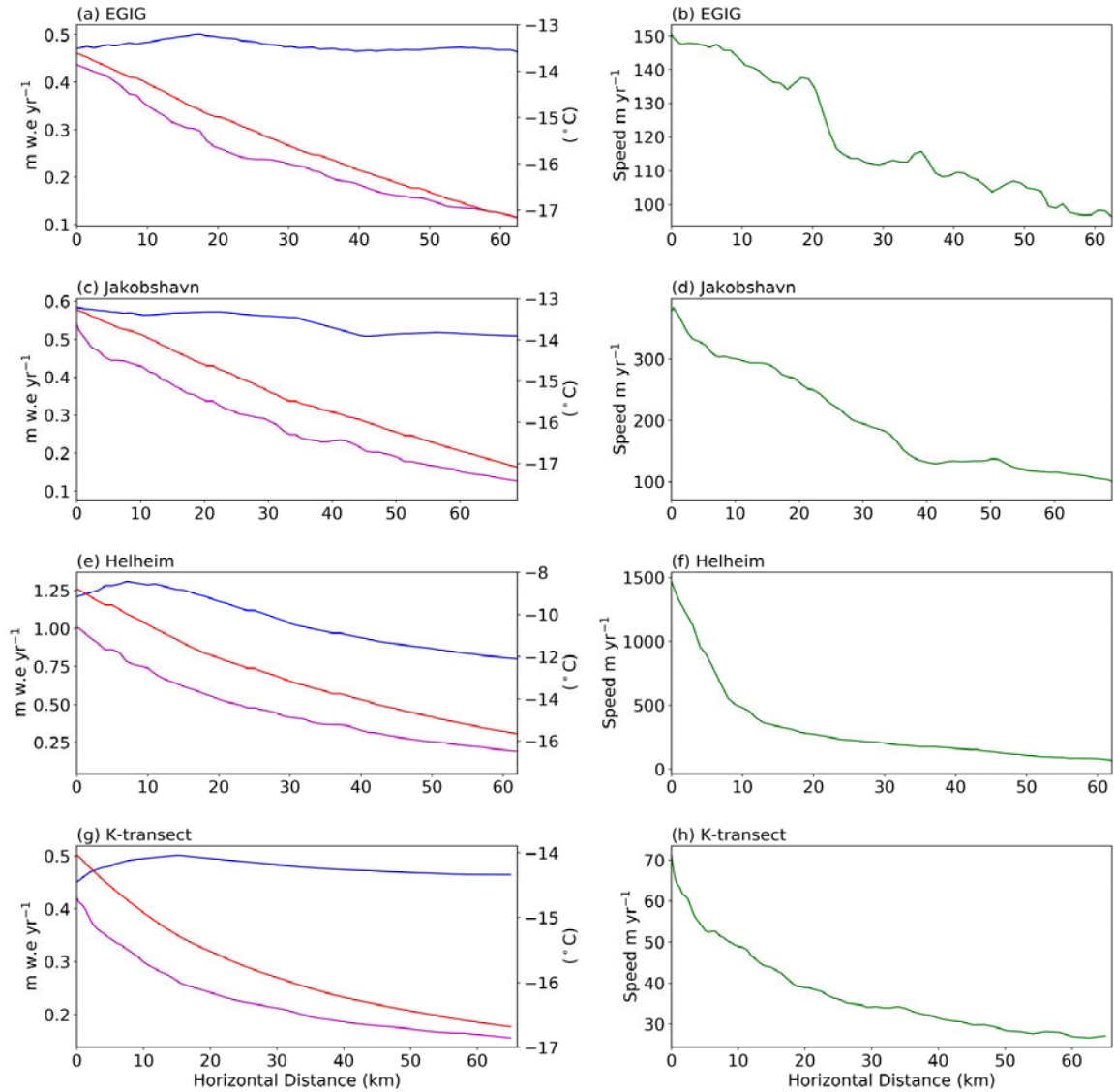
115



120

**Figure S2.** Modeled percent differences for sensitivity test forcings using dry model (black), Reeh model (red), bucket model (blue), and continuum model (green). Left panels show percent difference in air content and right panels show percent differences in temperature. (a-b) show results from varying horizontal velocity, (c-d) represent testing of variable accumulation rates, and (e-f) show results for different melt rates.

125



130 **Figure S3.** Surface conditions used for transect simulations. Left column shows snowfall (blue), temperature (red), and melt (magenta) extracted from RACMO2.3p2 (Noël et al., 2018) for 1980-2016 average. Right column shows snow speed extracted from (Joughin et al., 2010). Transects: EGIG (panels a,b); Jakobshavn (panels c,d); Helheim (panels e,f); K-transect (panels g,h).

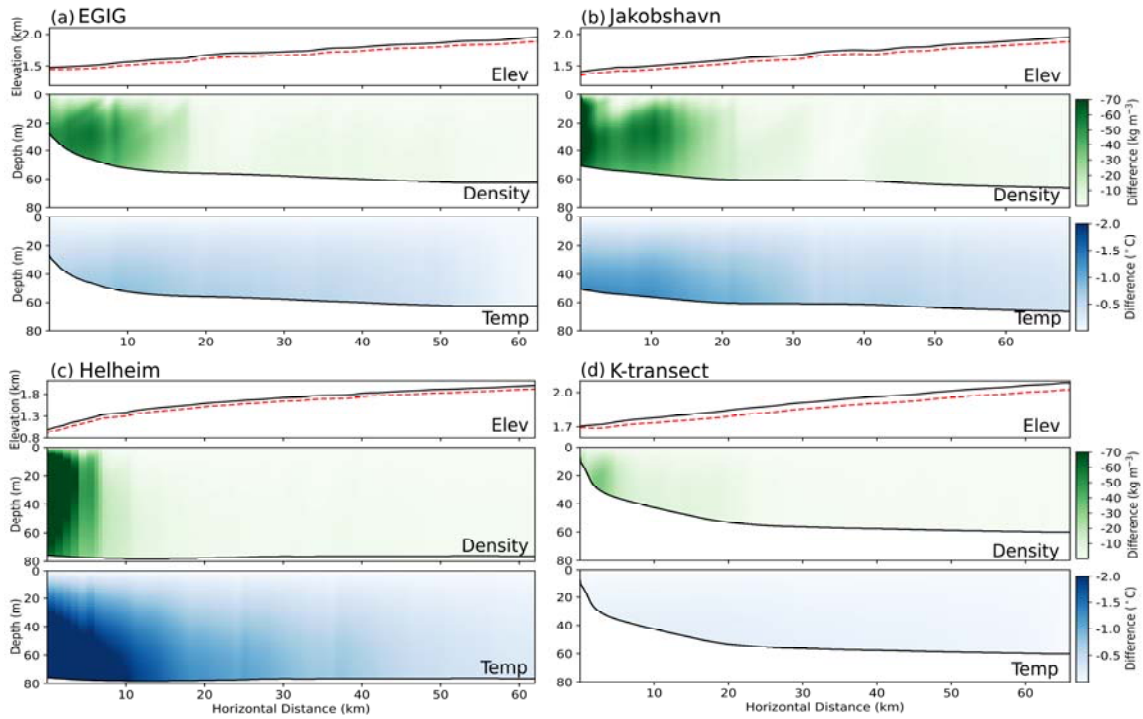


**Figure S4.** Modeled density and temperature differences between 1D and 2D results

140 using the Reeh et al. (2005) infiltration scheme at the EGIG (a), Jakobshavn (b), Helheim  
(c), and K-transect (d). Top panel in each shows surface topography (black line) and 2D  
modeled depth to pore close-off (dashed red line).

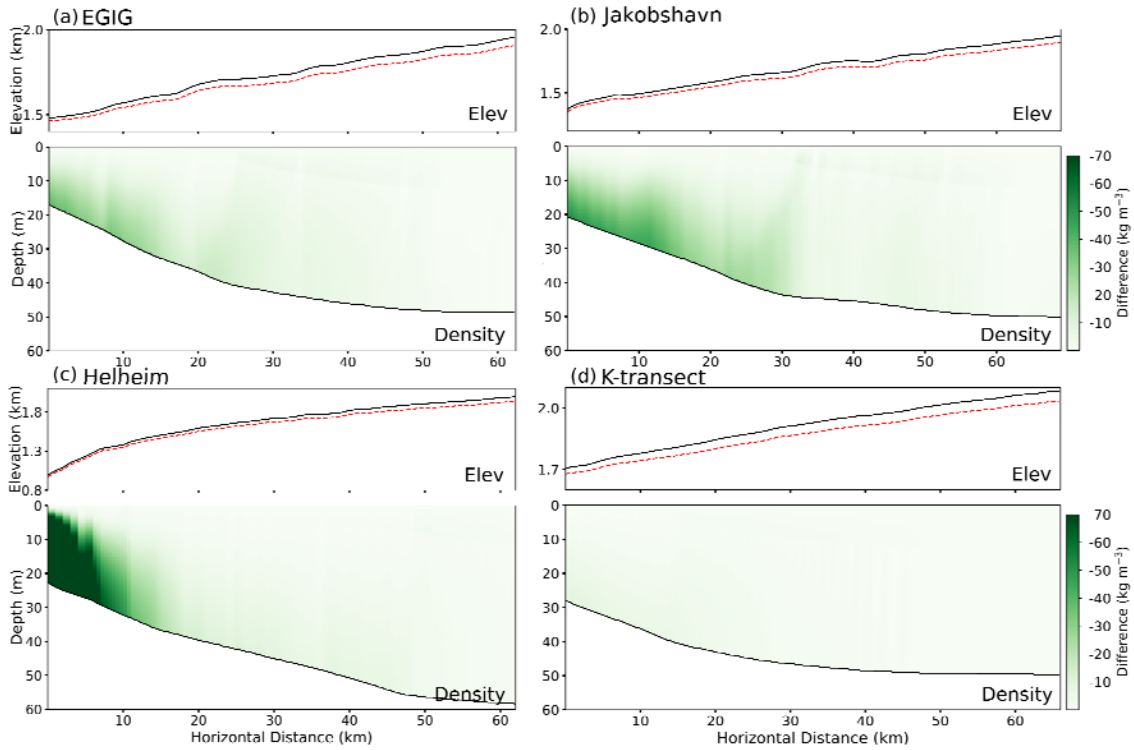


**Figure S5.** Modeled density differences between 2D and 1D simulations for GrIS

145 transects as in Figure S3, but for the continuum meltwater infiltration scheme. Continuum  
 model results were found to be insensitive to temperature (Figure S2) and are not  
 displayed.

150

## References

- Alley, R. B. and Bentley, C. R.: Ice-Core Analysis on the Siple Coast of West Antarctica, *Ann. Glaciol.*, 11, 1–7, doi:10.3189/s0260305500006236, 1988.
- Harper, J., Humphrey, N., Pfeffer, W. T., Brown, J. and Fettweis, X.: Greenland ice-sheet contribution to sea-level rise buffered by meltwater storage in firn, *Nature*, 491(7423), 240–243, doi:10.1038/nature11566, 2012.
- Joughin, I., Smith, B. E., Howat, I. M., Scambos, T. and Moon, T.: Greenland flow variability from ice-sheet-wide velocity mapping, *J. Glaciol.*, 56(197), 415–430, doi:10.3189/002214310792447734, 2010.
- Koenig, L. S., Miège, C., Forster, R. R. and Brucker, L.: Initial in situ measurements of perennial meltwater storage in the Greenland firn aquifer, *Geophys. Res. Lett.*, 41(1), 81–85, doi:10.1002/2013GL058083, 2014.
- Meierbachtol, T., Harper, J. and Johnson, J.: Force balance along isunnguata Sermia, west Greenland, *Front. Earth Sci.*, 4(September), 1–9, doi:10.3389/feart.2016.00087, 2016.
- Noël, B., Van De Berg, W. J., Van Wessem, J. M., Van Meijgaard, E., Van As, D., Lenaerts, J. T. M., Lhermitte, S., Munneke, P. K., Smeets, C. J. P. P., Van Uft, L. H., Van De Wal, R. S. W. and Van Den Broeke, M. R.: Modelling the climate and surface mass balance of polar ice sheets using RACMO2 - Part 1: Greenland (1958-2016), *Cryosphere*, 12(3), 811–831, doi:10.5194/tc-12-811-2018, 2018.
- Reeh, N., Fisher, D. A., Koerner, R. M. and Clausen, H. B.: An empirical firn-densification model comprising ice lenses, in *Annals of Glaciology*, vol. 42, pp. 101–106., 2005.